Hydrogen tube vehicle for supersonic transport: 2. Speed and energy

Arnold R. Miller*
Vehicle Projects Inc and Supersonic Tubevehicle LLC
200 Violet St, Suite 100, Golden, CO 80401, USA

Abstract

The central concept of a new idea in high-speed transport is that operation of a vehicle in a hydrogen atmosphere, because of the low density of hydrogen, would increase sonic speed by a factor of 3.8 and decrease drag by 15 relative to air. A hydrogen atmosphere requires that the vehicle operate within a hydrogen-filled tube or pipeline, which serves as a phase separator. The supersonic tube vehicle (STV) can be supersonic with respect to air outside the tube while remaining subsonic inside. It breathes hydrogen fuel for its propulsion fuel cells from the tube itself. This paper, second in a series on the scientific foundations of the supersonic tube vehicle, tests the hypothesis that the STV will be simultaneously fast and energy efficient by comparing its predicted speed and energy consumption with that of four long-haul passenger transport modes: road, rail, maglev, and air. The study establishes the speed ranking STV >> airplane > maglev > train > coach (intercity bus) and the normalized energy-consumption ranking Airplane >> coach > maglev > train > STV. Consistent with the hypothesis, the concept vehicle is both the fastest and lowest energy-consuming mode. In theory, the vehicle can cruise at Mach 2.8 while consuming less than half the energy per passenger of a Boeing 747 at a cruise speed of Mach 0.81.

Keywords: Energy consumption, fuel cell, hydrogen, speed, supersonic transport

1. Introduction

The hydrogen tube vehicle is a new idea in supersonic transport. The central concept is that operation of a vehicle in a hydrogen atmosphere, because of the low density of hydrogen, would increase sonic speed and dramatically decrease drag relative to air [1]. A hydrogen atmosphere requires that the vehicle operate in a hydrogen-filled tube or pipeline. To prevent leakage of air into the tube, hydrogen pressure is slightly above outside air pressure, and the tube serves as a phase separator. Mach 2.8 in air corresponds to only Mach 0.74 in hydrogen, the ratio of the speed of sound in the two phases, and thus the vehicle can be supersonic with respect to air outside the tube while remaining subsonic inside. Operating with respect to two gas phases, the vehicle has two Mach numbers. Because energy consumption is a function of the first power of gas density, the hydrogen atmosphere should reduce energy consumption at a given speed by a factor of 15 relative to air of the standard atmosphere at zero altitude.

The proposed supersonic tube vehicle (STV) is a cross between a train and an airplane. Like a train, it is multi-articulated and, runs on a guideway within the tube. Like an airplane, it is propelled by contra-rotating propfans and levitates or flies on hydrogen aerostatic gas

* Corresponding author. Tel.: +1 303 296 4218; fax: +1 303 296 4219
Email address: arnold.miller@vehicleprojects.com (Arnold R. Miller)
Additional information: www.ArnoldRMiller.net

bearings. Fig. 1 depicts the front locomotive and first railcar of a trainset. Onboard hydrogen-oxygen fuel cells provide propulsion power. The vehicle breathes hydrogen fuel from the tube itself, carries liquid oxygen (LOX) onboard, and collects and stores the product water until the end of a run. Breathing fuel from the tube solves the problem of hydrogen storage, a major challenge of contemporary hydrogen fuel-cell vehicles.

The first paper in this series, whose collective objective is to analyze the scientific foundations and feasibility of the supersonic tube vehicle[1], addressed several aspects of feasibility [1]: It (a) mathematically established vehicle power at supersonic speed with respect to air; (b) as depicted in Fig. 2, showed that the vehicle can carry sufficient LOX and water to make a nonstop supersonic transcontinental run of 3960 km; (c) discussed hazard scenarios; (d) presented a method of propfan bidirectional propulsion and braking; and (e) listed or discussed a dozen open issues facing realization of the concept.

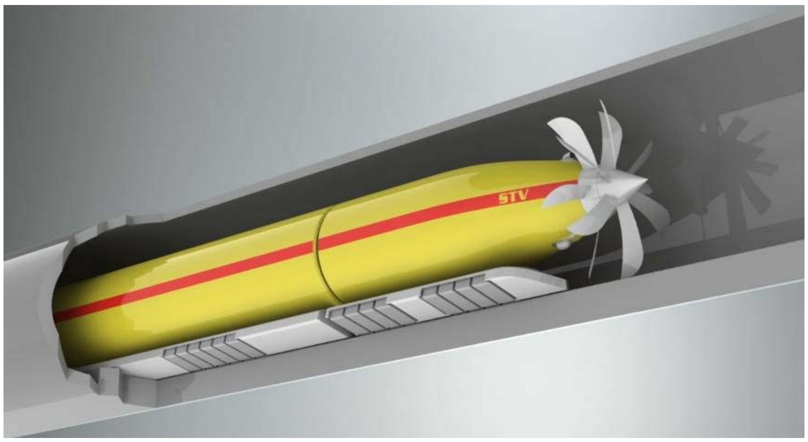

Fig.1. Supersonic tube vehicle (STV) in its hydrogen tube: Cutaway CAD model shows propulsion by contra-rotating propfans and levitation on aerostatic gas bearings. Fuselage outer diameter is 2.69 m, and tube inside diameter is 6.4 m. Tube hydrogen pressure is slightly above outside air pressure.

This paper, second in the series, tests the hypothesis that the STV will be simultaneously fast and energy efficient. Because "fast" and "efficient" are relative descriptions, the paper tests the hypothesis by comparing the theoretical speed and energy consumption of the STV with empirical values for four conventional long-haul passenger transport modes: road, rail, maglev, and air. If the STV is shown not to be simultaneously fast and energy efficient, then pursuing costly development of hardware prototypes, as an early step toward commercialization, would not be warranted.

[1] Topics covered by the planned series, with main title "Hydrogen Tube Vehicle for Supersonic Transport," include (a) the concept and preliminary feasibility, (b) comparison of speed and energy with other transport modes, (c) aerodynamics in hydrogen, (d) total cost -- the sum of infrastructure, operating, maintenance, and social costs – and (e) hazard analysis, including flammability and intra-tube noise. The first paper of the series [1], though not numbered in its title, focused on the vehicle concept and its validation but also addressed in a preliminary manner engineering-design issues such as a seating arrangement in a passenger car, engineering challenges facing gas-bearing levitation, methods of removing air or water inadvertently introduced into the tube hydrogen, and the optimum ratio of vehicle diameter to tube diameter. The paper at hand, second in the series, is derived from a conference-proceedings paper [2]. The third paper, "Hydrogen tube vehicle for supersonic transport: 3. Aerodynamics in hydrogen" [3], includes analysis of propeller efficiency in hydrogen, increased aerodynamic drag due to accelerated gas flow in the gap between vehicle outer surface and tube inner surface, and Mach waves in a hydrogen tube. Following this series on scientific foundations and feasibility, a second series of papers will address engineering analysis and design.

Empirical data are obtained for typical examples of vehicles serving each long-haul passenger mode and include Prevost® X3-45 and other intercity coaches for road transport, Siemens ICE 3®/Velaro® high-speed train for rail, Siemens/ThyssenKrupp Shanghai Transrapid for maglev, and Bombardier Q400 turboprop and Boeing 747 turbofan aircraft for air transport.

In this study, I will show that the STV can, in principle, cruise at Mach 2.8 and concurrently consume less than half the energy per passenger of a Boeing 747 at a cruise speed of Mach 0.81.

2. Analysis of Speed

All of the modes experience an ultimate aerodynamic limit of speed determined by onset of the transonic region, Mach 0.8 – 1.2. As a vehicle enters the region, airflow over its surface is a mixture of subsonic and supersonic flow, and it encounters the power peak and dynamic instability that constitute the *sound barrier*. Maglev, aircraft, and the STV may indeed experience a transonic limit of speed; however, the other two modes – road and rail – encounter distinct theoretical limits at speeds lower than the transonic limit. All modes except airplanes and the conceptual STV encounter practical limits below the theoretical limits.

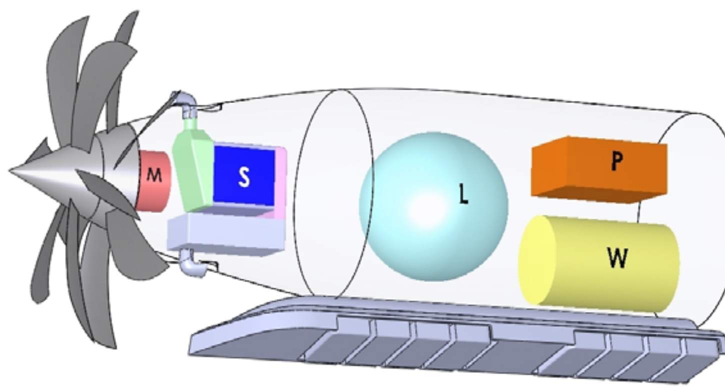

Fig 2. X-ray view of an STV locomotive: As treated in the original paper [1], this drawing shows feasibility of packaging essential components onboard for supersonic transit: (a) fuel-cell stacks of the required power; (b) LOX storage to allow nonstop transcontinental operation; and (c) water produced during the run. The components shown are M = propulsion motors, S = fuel-cell stacks, L = LOX storage system, P = power electronics, and W = water holding tank. Components S, L, and W are to the scale of the fuselage diameter of 2.69 m.

Table 1 displays the estimated practical speeds for all five modes.

2.1 Road Transport

The flexibility of pneumatic rubber tires gives relatively quiet and cushioned levitation, guidance, propulsion, and braking, and the flat contact patch at the interface of the tire and road provides good wheel adhesion. However, the flat contact patch results in the tire radius directly above being smaller than the nominal radius of the tire. The consequence of the constant change in radius as the tire rolls is flexing work, internal friction, and temperature rise in the rubber. The resistive force caused by these effects of tire deformation is termed *rolling resistance*. Rolling resistance increases linearly with weight and more than the second power of speed [4]. At high speed, dynamic instability – a standing wave in the tire carcass behind the contact patch – results in catastrophic tire failure. A sixth-order partial differential equation [5] satisfactorily models a radial tire as a cylindrical shell (the belt) connected to the axle by springs (the sidewalls). The model agrees well with experiment [5] and predicts that the amplitude of tire vibrations becomes unbounded when rotational speed Ω exceeds the range set by the inequality

$$\Omega \leq [q / (\rho a^2 h)]^{1/2} \quad (1)$$

where Ω is tire rotational speed (in rad/s), q is the normalized torsional modulus of elasticity of the belt (N m^3 rad^{-1}), ρ is density of the cord-rubber tread material (kg m^{-3}), a is mean belt radius, and h is belt thickness. Equation (1) implies a distinct upper limit on vehicle speed of pneumatic rubber-tired road vehicles. For reasons such as short life, harsh ride, high energy consumption, and unsafe performance on wet pavement, practical rubber tires for a coach (intercity bus) would limit its sustained maximum cruise speed to lower values than the theoretical limit of Eq. (1).

The most compelling limit to the practical speed of coaches is the posted freeway speed limit, in the range 100-150 km/h, which is the result of sharing the road with slow traffic, poor road conditions, unbanked curves, and acoustic noise at ground level. We will take 150 km/h as the practical limit of conventional coach speed. To exceed this value would require a dedicated infrastructure restricted to fast vehicles and possessing banked curves.

2.2 Rail Transport

In conventional high-speed rail, levitation, guidance, propulsion, and braking are provided by steel wheels on steel rails. Rolling resistance is minimal; however, as a trade-off, tractive effort and braking force are often determined by wheel adhesion rather than torque. Conventional guidance utilizes *conical guidance*: Each wheel is a section through a cone, with the smaller diameter to the outside, and the two wheels of a wheelset are connected by a rigid axle. If, for instance, the vehicle moves to the right on straight rails, the right-hand wheel effectively has a larger diameter than the left; consequently, the vehicle automatically steers back to the left. The wheel flanges blend into the cone but are mainly required in sharp curves, in which the flanges enforce guidance. Flange guidance is undesirable because of high friction and noise.

Conical guidance results in a hunting phenomenon termed *Klingel oscillations*, whose wavelength, based on geometrical considerations, is given by the equation

$$\lambda = 2\pi (r g / \theta)^{1/2} \quad (2)$$

where λ is wavelength, r is wheel radius, g is half the distance between contact points on adjacent rails, i.e., half the track gauge, and θ is the conicity or angle of inclination of the cone [6]. Because wavelength is constant, Eq. (2) implies that kinematic vibration frequency will increase as the first power of vehicle speed. If unchecked, Klingel oscillations can lead to chaotic oscillations and result in derailment. Chaotic wheelset oscillations have been demonstrated and studied both experimentally and by computer simulation [7]. Equation (2) describes a theoretical speed-limiting phenomenon of conventional, conical-guidance railway vehicles. The limit, however, is not a definite, firm limit like that set by standing waves in rubber tires or the sound barrier for aircraft, and the limit of speed is determined by how much vibration is tolerable. The world's conventional-train speed record of 575 km/h was set by a specially prepared 18.6 MW TGV on new track infrastructure. In view of the intense vibration and noise of the run, it was proposed that 350 km/h is a practical limit [8]. The tolerable upper limit for kinematic oscillations probably lies between 350 and 575 km/h.

For catenary-electric trains, travelling mechanical waves on the catenary line also limit speed, possibly to lower values than Klingel oscillations [9]. Unlike kinematic oscillations, this represents a well-defined limit, namely, the speed at which the pantograph reaches the propagation speed of the wave. At the propagation speed, the wave becomes a standing wave with respect to the train.

The above notwithstanding, practical lower limits on speed of rail transport are imposed by (a) aerodynamic noise generated by high-speed operation at ground level, and indeed, conventional high-speed trains, cruising at 300 km/h, can result in supersonic air velocity in tunnels and a sonic boom emanating from the tunnel exit [10]; (b) the need for adequate braking distance because of the braking limit imposed by wheel adhesion rather than torque; (c) wheel and rail wear, which is exacerbated by constant exposure to dirt, sand, and the elements; (d) inadequate rail infrastructure, including lack of rail straightness and levelness and the use of unbanked curves; (e) sharing of the railway with slower freight traffic, which impose traffic hazards and cannot operate on banked curves.

Most high-speed passenger trains today, for example, the Japanese Shinkansen, French TGV, and German ICE, can operate continuously at 300 km/h. Nonetheless, they frequently operate at lower speeds because of practical limitations (a) – (e) listed above. Currently, the fastest revenue-service train is the Chinese CRH3, which can operate at up to 350 km/h on a line between Beijing and Tienjin, a distance of 115 km [11]. An essential contributor to high operating speed is the track infrastructure, which uses a 100 km concrete viaduct as foundation [12]. I propose using the 350 km/h of the Chinese CRH3 as the practical limit for conventional passenger rail. To make this a practical limit on most rail systems in the world would require new track infrastructure.

2.3 Maglev Transport

The only maglev train currently operating in revenue service is the Transrapid, an EMS (electromagnetic suspension), long-stator type with stator segments of about one-kilometer length [13], deployed as a shuttle train at the Shanghai airport, and it is the one we will analyze in this study. The run from the Pudong Airport to the outskirts of Shanghai, a distance of 30 km and requiring 7.3 minutes, operates for a fraction of a minute at its cruise speed of 430 km/h, with the balance of transit time taken by acceleration and deceleration.

Maglev trains experience no counterpart to the kinematic vibration or catenary-wire travelling waves of high-speed rail. However, onset of the transonic region, at about 980 km/h at sea level, sets a definite upper limit on speed. Because of interaction of the airstream with the guideway and ground, the aerodynamic limit is below this.

Presumably because of high capital cost of the long stator, maglev has only been implemented, since 2003, in the short 30 km run of the Shanghai airport shuttle, and limited operational data are available. Practical speed-limiting factors should overlap with those for high-speed rail. In any case, the Shanghai maglev has been demonstrated at 500 km/h, and we will take that speed as the practical upper speed limit for technology implemented today.

2.4 Air Transport

Today, the fastest mode of transport is the airplane. Because of the high energy consumption and noise of supersonic flight, however, the speed of conventional air transport is limited by the speed of sound in air. Entering the transonic region, the airplane encounters a power peak due to orthogonal Mach waves, or shock waves, and experiences dynamic instability from movement of the waves on its surface. Beyond the transonic region, it requires high power to drive oblique Mach waves, the cause of sonic booms, and power rises faster than the cube of speed. The Concorde supersonic transport suffered several challenges: sonic booms, high-altitude air pollution, low passenger capacity, short range, and high energy consumption; in fact, fuel consumption in the supersonic region at the rate of 25 600 L/h was a major contributor to its demise [14].

One of the most successful passenger airplanes, the Boeing 747-400, can cruise at Mach 0.85 at an altitude of 10 600 m [15]. Because the speed of sound in the standard atmosphere at that altitude is 1070 km/h, we will take 910 km/h as today's practical speed limit of air transport.

2.5 STV Transport

In a sufficiently large tube, the maximum speed of the supersonic tube vehicle is the speed at which the propeller-blade tips enter the transonic region in hydrogen. Speed of a blade tip, which traces out a helix as the vehicle advances, is greater than vehicle speed because a component of rotational velocity adds to vehicle translational velocity. Propfans, which approach 90 % efficiency in practice, allow higher vehicle speed than conventional propellers by using sharp-edged, swept-back blades like supersonic wings (see Fig. 3).

Fig. 3. State-of-the-art Antonov propfan airplane: Analysis of the maximum cruise speed of the propfan-driven STV is based on aerodynamic extrapolation of the cruise speed (Mach 0.74) of the 41 MW, 145 t Antonov An-70 (photo source: Oleg Belyakov).

We will estimate the practical maximum cruise speed of the STV when using propfan propulsion from the speed of the 41 MW, 145 t Antonov An-70 (Fig. 3), a state-of-the-art contra-rotating turbo-propfan transport aircraft. The estimated short-range cruise speed of the An-70 is 800 km/h at an altitude of 9100-11 000 m [15]. For the purpose of calculation, I use the midpoint cruise altitude of 10 050 m. Because the speed of sound at that altitude in the standard atmosphere is 1080 km/h, the speed of the An-70 is Mach 0.74. Assuming the Mach number for the onset of the transonic region for the blade tips in hydrogen is the same as that in air, the maximum cruise speed of the STV should be larger than that of the An-70 by the ratio of the speed of sound in hydrogen at 1 bar (4720 km/h) to its speed in air at 10 050 m (1080 km/h). Thus, the maximum cruise speed of the STV is estimated as $(4720 \text{ km h}^{-1}/1080 \text{ km h}^{-1}) \cdot 800$ km/h = 3500 km/h (Mach 0.74) in hydrogen, which corresponds to Mach 2.8 in air at sea level outside the tube.

Acoustic noise at ground level is not an issue for the STV because the vehicle by necessity operates within a tube. Noise inside the tube, however, may be an issue.

3. Analysis of Energy Consumption

The dominant contributor to energy consumption for all five transport modes is aerodynamic drag. For a subsonic vehicle in a free gas (that is, with no flow interference from the ground or other objects), all drag aside from lift is termed *parasitic drag* and is given by

$$D_p = ½\, C_p\, A\, \rho\, V^2 \quad (3)$$

where C_p is the drag coefficient, A is the frontal (or other) area of the vehicle, ρ is gas density, and V is vehicle speed [16]. Parasitic drag is the sum of predominantly *pressure drag* and *skin-friction drag*. For a land vehicle, interference of the airstream with the ground and flow under the vehicle make Eq. (3) a lower bound on aerodynamic drag.

When a free-gas vehicle is in equilibrium at a fixed speed V_0, its required thrust $F = D_p$. Therefore, its required power to overcome parasitic drag is $P = F\, V_0$ and

$$P = ½\, C_p\, A\, \rho\, V_0^{\,3} \quad (4)$$

and power increases as the cube of vehicle speed. Because propulsion energy E to overcome vehicle drag is $E = F\, d_0$, where F is force (drag) and d_0 is a fixed distance, the energy consumption for the vehicle to traverse d_0 at constant speed V_0 is $E = D_p\, d_0$, and

$$E = D_p\, d_0 = ½\, C_p\, A\, \rho\, d_0\, V_0^{\,2} \quad (5)$$

Therefore, energy consumption increases as the square of speed.

We will consider energy consumption for the vehicle alone, ignoring upstream energy losses. In conventional comparisons of the energy consumption of passenger transport vehicles, the raw energy E_0 to carry N_0 passengers a fixed distance d_0 at a level grade and fixed speed V_0 is "Nd-normalized" as shown by the following equation

$$E_{Nd} = E_0 / (N_0\, d_0) \quad (6)$$

where E_{Nd} is the Nd-normalized energy consumption, which is often termed the specific secondary energy consumption. We will assume that all seats in a vehicle are occupied, and hence N_0 is either the number of passengers or equivalently the number of seats. Nd-normalized energy E_{Nd} has the units kJ (seat km)$^{-1}$.

While we will use Nd-normalization in this analysis, it has the deficiency of penalizing fast vehicles. If a coach and airplane have the same N_0 and d_0 values, the airplane will have higher E_0 because it travels at higher speed and energy consumption due to aerodynamic drag rises as the square of speed (see above). Nonetheless, in passenger transport, high speed, and hence minimum time, is a benefit that should be recognized in energy normalization. I therefore define "NV-normalized" energy as

$$E_{NV} = E_0 / (N_0\, V_0) \quad (7)$$

where V_0 is the vehicle speed in km/h at which E_0 was measured. Equation (7) is equivalent to multiplying Equation (6) by t_0, where t_0 is the time in hours to traverse distance d_0 at speed V_0. From Equation (7), we have

$$E_{NV} = E_0 / (N_0\, d_0\, t_0^{-1}) = E_0\, t_0 / (N_0\, d_0) = E_{Nd}\, t_0 \quad (8)$$

and E_{NV} has the units kJ h (seat km)$^{-1}$. I propose that NV-normalization compensates, in part, for a bias against fast vehicles by use of Nd-normalization alone.

Table 2 collects the energy-consumption results for all five modes.

3.1 Road Transport

The drag coefficient C_p of coaches is high because their length is limited by the steering demands of and traffic on the two-dimensional road network. They are aerodynamic bluff bodies because they have broad, flattened fronts and backs. Moreover, each vehicle receives the full brunt of pressure drag. In contrast, segmented vehicles in which segments are assembled into long, articulated vehicles, or trains, have each segment protected from the full force of pressure drag by the preceding segment. Although long vehicles have higher skin-friction drag than short vehicles, pressure drag is more significant for low-subsonic vehicles.

Table 3 displays empirical data for typical coaches. A manufacturer [17] provided one set of data, and coach operators [18, 19] provided the other two sets. The collective data represent at least two brands of coaches. The data are so similar for the three cases that we use the mean of the three as values for the number of seats N_0, cruise speed V_0, and fuel consumption in volume per distance.

Mean seating capacity N_0 = 55. After converting units, mean speed (corresponding to the energy measurement E_0) is V_0 = 110 km/h and diesel-fuel consumption is 0.362 L/km. Taking the energy content of diesel fuel as 38.6 MJ/L, the energy per kilometer is 14.0 MJ/km. Normalizing further by N_0 gives E_{Nd} = 254 kJ (seat km)$^{-1}$. The time to traverse 1.0 km at a fixed speed of V_0 is 0.00914 h, and E_{NV} = [254 kJ (seat km)$^{-1}$] · (0.00914 h) = 2.32 kJ h (seat km)$^{-1}$.

3.2 Rail Transport

High-speed trains approximate the aerodynamic ideal of being long, slender, and pointed at each end. Moreover, as noted above, each rail car shields the subsequent car from full pressure drag.

For empirical data, we use the data, based on empirical results and computer simulation, provided in a report by Dornier Consulting [20]: For an ICE 3 train operating at a constant speed of V_0 = 300 km/h, with N_0 = 415 seats, over a fixed, level-grade distance of d_0, the Nd-normalized energy is E_{Nd} = 51 W h (seat-km)$^{-1}$. Converting units, this corresponds to E_{Nd} = 184 kJ (seat km)$^{-1}$. The time to traverse 1.0 km at 300 km/h is 0.00333 h, and the E_{NV}-normalized energy at the overhead contact wire is $E_{Ndt} = E_{Nd}\, t_0$ = 0.612 kJ h (seat km)$^{-1}$.

3.3 Maglev Transport

The difference between the energy consumption of an EMS maglev train and a conventional high-speed train is not large. While no mechanical friction accompanies magnetic levitation, energy is dissipated by electromagnet excitation, which is exacerbated by the large air gap of 1 cm in current practice. To accommodate the levitation system, the maglev train is wider than an ICE 3 train and has more bluff-body character.

To compute the energy for consistent comparison with the other transport modes, we need the energy at the interface of the electric power grid and electrical substation that provides all energy to the Transrapid train – including internal vehicle operations, levitation, and propulsion by the long stator – when it operates at constant speed over a fixed, level-grade distance. The Shanghai Transrapid has V_0 = 430 km/h and N_0 = 446 seats in a five-section train. Based on empirical data and computer simulation, Dornier Consulting [20] has recommended an Nd-normalized energy of 63 W h (seat km)$^{-1}$. Conversion of units gives E_{Nd} = 227 kJ (seat km)$^{-1}$. The time to traverse 1.0 km at 430 km/h is 0.00233 h, and the NV-normalized energy at the grid/substation interface is $E_{\mathrm{NV}} = E_{\mathrm{Nd}}\, t_0$ = 0.527 kJ h (seat km)$^{-1}$.

3.4 Air Transport

Besides parasitic drag, airplanes suffer high energy consumption, half of the total, from levitation by wings. Wings have the function of diverting a large mass of air to downwash, i.e., downward flowing air behind the wing. Newton's third law states that the lift on the airplane equals the vertical component of the force vector to effect downwash. The required force on the air to create downwash is termed *induced drag* and is given by the equation

$$D_{\mathrm{i}} = \mathrm{C_i}\, W^2 / (½\, b^2 \rho\, V^2) \qquad (9)$$

where $\mathrm{C_i}$ is the induced-drag coefficient, which depends on the shape of the airfoil and angle of attack, W is aircraft weight, b is wing span, ρ is air density at altitude, and V is vehicle speed [16]. Wing span b, for a given airfoil, is a measure of wing surface area, and the larger the wing area, the lower the induced drag: Greater mass of air is diverted, and because kinetic energy equals ½ $m\, v^2$, where v is the vertical component of downwash velocity, lower kinetic energy is imparted to the downwash. If the wing area were infinite, induced drag would be zero [21]. However, the larger the wing area, the higher the parasitic drag, and when a subsonic airplane is minimized for total drag, induced drag equals parasitic drag [16]. The W^2 factor in the numerator of Eq. (9) makes cargo aircraft especially energy consuming.

For energy consumption of passenger air transport, we will analyze a Boeing 747-400 and Bombardier Dash 8 Q400. The Boeing 747-400 was chosen because its average seating capacity of 371 seats (see Table 4) rivals the capacity of high-speed trains, and it is arguably the most commercially successful long-haul jet transport. The Bombardier Q400 is a modern, efficient, midsized turboprop aircraft that I analyzed in the first paper of the series [1]; by design, the STV has the same fuselage diameter as the Q400.

The Boeing 747-400 empirical data are for 4773 flights, averaging 7690 km each, between the United States and Asia/Oceania or within Asia/Oceania in the third quarter of 2008 [22]. They comprise the entire flights for the quarter in that geographical region by two US carriers, and the sampling error is negligible. Because of the large number of flights throughout the region, we believe individual variation in winds and cruise altitude are cancelled to give an accurate representation of the cruise conditions. Because of the long flight durations, our methods of calculation of speed and fuel consumption, dictated by available data, introduce small deviations from the true cruise conditions, and statistical-bias errors are estimated as 1-3 % [22]. Mean speed is calculated by dividing the gate-to-gate distance aggregated by origin-to-destination (for example, all flights from Chicago to Beijing by a single carrier) by the analogously aggregated takeoff-to-landing time. Mean fuel consumption per seat is calculated by dividing the gate-to-gate fuel consumption aggregated by all 4773 flights by the total number of seats in all 4773 flights. Although distance, time, and fuel are required by taxiing, climb out, and descent, we believe the long flight durations reduce these operations to a small part of the overall distance, time, and fuel requirements. Because of the relatively slow speed of climb and descent, the calculated cruise speed will be lower than the true value; because of the large fuel consumption of a fully-fueled, long-haul aircraft in climb-out, the calculated cruise fuel consumption will be higher than the true value. The empirical data values are displayed in Table 4.

The Bombardier Dash 8 Q400 data are for 23 758 flights, averaging 462 km each, within the US mainland for the third quarter of 2008. They are the entire flights for the quarter in that geographical region by one US carrier, and sampling error is negligible. Flights were generally from small airports, and ground time is relatively short. The same considerations and methods of calculation as used for the Boeing 747-400 are used to calculate mean speed and mean fuel consumption per seat, and they introduce similar estimated statistical-bias errors of 1-3 %. The empirical data are reported in Table 4.

Energy consumption for the Boeing 747-400 is calculated from the data of Table 4, converted to metric units, with the energy content of Jet A fuel (kerosene) taken as 36.8 MJ/L. Mean fuel consumption per seat is 319 L/seat, and dividing by the mean flight distance of 7690 km gives the Nd-normalized energy as E_{Nd} = 1530 kJ (seat km)$^{-1}$. The time to traverse 1.0 km at 870 km/h is t_0 = 0.00115 h. Hence, $E_{\mathrm{NV}} = E_{\mathrm{Nd}}\, t_0$ = 1.76 kJ h (seat km)$^{-1}$.

Energy consumption for the Q400 is computed similarly from the data of Table 4. Mean fuel consumption per seat is 18.2 L/seat, and dividing by the mean flight distance of 462 km gives the Nd-normalized energy as E_{Nd} = 1450 kJ (seat km)$^{-1}$. The time to traverse 1.0 km at 481 km/h is t_0 = 0.00208 h. Hence, $E_{\mathrm{NV}} = \mathrm{E}_{\mathrm{Nd}}\, t_0$ = 3.02 kJ h (seat km)$^{-1}$.

3.5 STV Transport

As in the original STV analysis based on the Q400 airplane [1], energy consumption is calculated as $E_0 = P_0\, t_0$, where P_0 was estimated by aerodynamic analysis of the Q400 in air and in hydrogen [1, 23]. Speed V_0 of 1500 km, the minimum speed to be supersonic with respect to air outside the tube, and a three-segment trainset, two locomotives and one passenger car (see Fig. 1), are used in the following calculations because they were used in the original aerodynamic analysis. For one passenger car, we have N_0 = 74 and V_0 = 1500 km/h, d_0 = 3960 km, and E_0 = 3.8 x 10^4 MJ. Hence, Nd-normalization gives E_{Nd} = 130 kJ (seat km)$^{-1}$. At V_0 = 1500 km/h, the time to traverse 1.0 km is 0.000666 h, and NV-normalization gives $E_{\mathrm{NV}} = E_{\mathrm{Nd}}\, t_0$ = 0.0865 kJ h (seat km)$^{-1}$.

4. Results and Discussion

The vehicles representing the transport modes analyzed in this paper are specific but typical instances of classes of vehicles. We believe it is more useful for our purpose to have specific, typical results than aggregated, generic results. Tables 1 and 2 compare the practical cruise speed and energy consumption, respectively, of the five modes of transport. Empirical energy results for aircraft are based on more than 28 000 data points, and because they represent all flights of three carriers during three months and over a large geographical region, sampling error is negligible. Limitations in the available categories of data parameters, however, cause estimated statistical-bias errors of 1-3 % [22].

Rather than theoretical capability, the practical limits of speed in Table 1 are usually determined by high energy consumption due to poor aerodynamics, poor-quality infrastructure, sharing the infrastructure with slower vehicles, or ground-level acoustic noise.

A dedicated highway infrastructure, with banked curves and noise barriers, could raise the road-vehicle cruise speed to the limit imposed by standing waves in pneumatic tires (Eq. 1). Likewise, a dedicated railway infrastructure could raise rail speed to a limit imposed by Klingel oscillations (Eq. 2) or catenary-wire travelling waves. Air transport is the only mode of the five that already has an infrastructure in place allowing operation at the theoretical limit of speed.

For speed, the five modes rank as shown in the continued inequality

STV >> airplane > maglev > train > coach (10)

Using propfan propulsion, the STV can cruise, in principle, at Mach 2.8 relative to air outside the tube. In contrast, the Boeing 747-400 can cruise at Mach 0.85 at 10 600 m, and the Concorde supersonic transport cruised at Mach 2.2 at an altitude of up to 18 900 m. Assuming a sufficiently large tube, the propeller blade tips entering the transonic region limits vehicle speed to Mach 0.74 in hydrogen.

Energy consumption by the STV is the lowest of the five modes. As shown in Table 2, under conventional seat-distance energy normalization, the STV at 1500 km/h consumes 8 % of the energy consumed by the Boeing 747-400 at 870 km/h (Mach 0.81).,Because energy consumption due to parasitic drag rises as the square of speed, at 3500 km/h (Mach 2.8) the STV would consume 44 % of the energy of the Boeing 747 at Mach 0.81. The Nd-normalized energy consumption for the 371-seat Boeing 747-400 airplane is only slightly greater than the value for the 74-seat Bombardier Q400. Because the value for either airplane greatly exceeds the Nd-normalized energy consumption of the other four modes, we will not separate the two in ranking Nd-normalized energy consumption, as given by the continued inequality

Airplane >> coach > maglev > train > STV (11)

Introduction of NV-normalized energy consumption, which compensates for an Nd-normalized bias against fast vehicles, changes the energy consumption ranking. Now, because of greater speed, the 747-400 experiences about half the NV-normalized energy consumption of the Q400. Indeed, the Q400 has the highest energy consumption of the five modes, whereas the 747-400 has lower normalized energy consumption than the coach. The STV at 1500 km/h consumes 3 % of the NV-normalized energy consumed by the Q400 turboprop at 480 km/h, and its energy consumption is 16 % of that for the next most energy-efficient mode, the maglev train. Because of the large difference in energy consumption of the two airplanes, denoting the Q400 as "turboprop airplane" and the 747-400 as "turbofan airplane," we will separate them for ranking of NV-normalized energy, as given by the continued inequality

Turboprop airplane > coach > turbofan airplane > train > maglev >> STV (12)

In view of the analysis sections above, it is not surprising that road transport is energy intensive, especially with NV-normalization, because of (a) losses in rolling resistance, which increase linearly with weight and more than the second power of speed, (b) poor aerodynamics, and (c) slow speed enforced by low-speed infrastructure. Because of the first-power dependence of rolling resistance on vehicle weight, truck freight would fare worse than the normalized energy-consumption results in Table 2. Maglev and high-speed trains are close in energy consumption: The maglev is higher under Nd-normalization but lower under NV-normalization. This is understandable because advantages of one offset advantages of the other: Maglev has negligible guideway friction but requires levitation power. Energy consumption of air transport is high because of induced drag, which increases as the second power of weight. Indeed, normalized energy consumption of air cargo is about 50 times greater than conventional freight railways [24]. Because the STV operates in a low-density, low-drag hydrogen atmosphere and has low levitation-energy requirements [1], it consumes the least normalized energy of the five modes of transport.

The results of this study are more than (a) the STV is theoretically the fastest or (b) it is the least energy consuming of the five modes of transport. The study shows that (a) and (b) are simultaneously true. This result is well-summarized by the finding that at 3500 km/h the STV would consume less than half the energy per passenger of the Boeing 747 at 870 km/h. It is the concurrence of high speed and low energy consumption – demonstrated by empirical comparison with four conventional modes of transport – that make the STV attractive as a passenger transport mode. Its most fitting application, similar to that of the supersonic Concorde, is operations where time minimization is important.

5. Conclusions

In speed, the closest rival of the supersonic tube vehicle is the airplane. In theory, the STV can cruise at Mach 2.8 relative to air outside the hydrogen tube. The Boeing 747, in comparison, can cruise at Mach 0.85, and the supersonic Concorde could cruise at Mach 2.2.

However, the STV consumes much less energy than high-speed airplanes. Under conventional seat-distance energy normalization, the STV at 1500 km/h, the lowest supersonic speed in air at sea level, consumes 8 % of the energy per passenger of the Boeing 747-400 at 870 km/h. At 3500 km/h (Mach 2.8), the STV would consume less than half the energy of the Boeing 747 at 870 km/h (Mach 0.81). With seat-velocity normalization, the STV at 1500 km/h consumes only 3 % of the energy consumed by the Q400 turboprop at 480 km/h. The aircraft empirical energy results are based on large data sets (more than 4700 points for the 747 and more than 23 700 for the Q400), with negligible sampling errors but estimated statistical-bias errors of 1-3 %. Thus, the aircraft empirical results are as statistically sound as one can expect [22] Of the five transport modes compared, only air transport has an infrastructure in place that allows vehicles to reach their theoretical limit of speed. Because of its predicted high speed and concurrent low energy consumption, the STV's most attractive role is long-distance passenger transport, and its closest competitor is the supersonic jet transport.

Although a promising new idea in transport, the STV concept requires better understanding of the aerodynamics of vehicles operating in a hydrogen atmosphere within a tube, and many engineering challenges confront the practicality of aerostatic gas-bearings as levitation devices. Aerodynamics in hydrogen is the subject of the third paper [3] of this series, "Hydrogen Tube Vehicle for Supersonic Transport."

Acknowledgements

I thank my research assistant Kristen A. Johnson for help with data collection and our chief design engineer, Kris S. Hess, for the renderings of the STV shown in Figs. 1 and 2. I gratefully acknowledge Michael Witt of Dornier Consulting for provision of energy data on high-speed rail and maglev transport.

References

[1] A. R. Miller, Hydrogen tube vehicle for supersonic transport: Analysis of the concept, Int. J. Hydrogen Energy. 33 (2008) 1995-2006.

[2] A. R. Miller, Supersonic hydrogen tube vehicle: Speed and energy comparisons with road, rail, air, and maglev transport. In: Proceedings of HYPOTHESIS VIII, Lisbon, Portugal, 1-3 April 2009.

[3] A. R. Miller, Hydrogen tube vehicle for supersonic transport: 3. Aerodynamics in hydrogen, to be submitted to the International Journal of Hydrogen Energy.

[4] T. D. Gillespie, Fundamentals of Vehicle Dynamics, Society of Automotive Engineers, Warrendale, PA, USA, 1992.

[5] Roy, T. K., A Mathematical Treatment of the Radial Tire Modeled as a Rotating Shell on an Elastic Foundation, Dissertation (Mechanical Engineering), Texas Tech University, Lubbock, 1977.

[6] A. H. Wickens, A history of railway vehicle dynamics. In: Simon Iwnicki (Ed.), Handbook of Railway Vehicle Dynamics. CRC Press, Boca Raton, FL, USA, 2006.

[7] K. Tanifuji and K. Nagai, Chaotic oscillation of a wheelset rolling on rail; verification on roller rig, Vehicle System Dynamics. 25 (1996) 682-693.

[8] French train breaks speed record. Associated Press, 4 April 2007. Website: (http://www.cnn.com).

[9] A. Bobillot, L. M. Cléon, A. Collina, O. Mohamed, R. Ghidorzi, Pantograph-catenary: A high-speed European couple. In: Proceedings of the Eighth World Congress on Railway Research 2008, Seoul, South Korea, 18-22 May 2008.

[10] B. Schulte-Werning, B. Asmussen, W. Behr, K. G. Degen, and R. Garburg, Advancements in noise and vibration abatement to support the noise reduction policy of Deuthsche Bahn. In: Proceedings of the Eighth World Congress on Railway Research 2008, Seoul, South Korea, 18-22 May 2008.

[11] Velaro sets Chinese speed record. Railway Gazette, 27 June 2008. Website: (http://www.railwaygazette.com/news_view/article/2009/05/9605/velaro_sets_chinese_speed_record.html).

[12] Beijing-Tianjin high-speed commuter link. Railway Technology, China, copyright 2009. Website: (http://www.railway-technology.com).

[13] H. Buethe, S. Le Dren, D. Steinbrink, P. E. Zamzow, and H. Maschik, Long stator winding cable for the MAGLEV propulsion of the Transrapid Shanghai Project. In: Proceedings of 52nd IWCS/Focus International Wire & Cable Symposium, Philadelphia, PA, USA, 17-20 November 2003.

[14] Air travel: A supersonic future? BBC News, UK, 17 July 2001. Website: (http://news.bbc.co.uk/2/low/uk_news/852087.stm).

[15] P. Jackson, (Ed.), Jane's All the World's Aircraft 2006-2007, Jane's Information Group, Alexandria, VA, USA, 2006.

[16] H. C. Smith, The Illustrated Guide to Aerodynamics, 2nd ed., TAB Books, Blue Ridge Summit, PA, USA, 1992.

[17] K. Elmers, Custom Coach Corp., Columbus, OH, USA, personal communication, 13 February 2009.

[18] G. Agnes, Ramblin Express, Colorado Springs, CO, USA, personal communication, 28 May 2009.

[19] G. Wordekemper, Arrow Stage Lines, Denver, CO, USA, personal communication, 27 May 2009.

[20] D. Rogg and M. Witt, Energy consumption of high speed railways, Dornier Consulting, Berlin, Germany, 22 May 2009 (report prepared for Vehicle Projects Inc).

[21] D. F. Anderson and S. Eberhardt, Understanding Flight, McGraw-Hill, New York, NY, USA, 2001.

[22] Analysis Review: Fuel consumption of Boeing 747-400 and Bombardier Q400 passenger airplanes, Boyd Group International, Evergreen, CO, USA, 11 June 2009 (report commissioned by Vehicle Projects Inc, Golden, CO, USA).

[23] A. R. Miller, "Beyond aircraft: Supersonic hydrogen tube vehicle." In: Proceedings of the World Hydrogen Technologies Convention, New Delhi, India, 25-28 August 2009.

[24] E. Hirst, Energy-intensiveness of transportation, J. Transp. Eng., Am. Soc. Civil Engineers. 99(1) (1973) 111-122.

Table 1 – Practical cruise speeds V_c

Mode	V_c km/h
STV	3500
Airplane	910
Maglev	500
High-Speed Train	350
Coach	150

Table 2 – Normalized energy consumption

Mode	E_{Nd} kJ (seat km)$^{-1}$	V_0 [a] km/h	E_{NV} kJ h (seat km)$^{-1}$
Airplane			
Boeing 747-400 [b]	1530	870	1.76
Bombardier Q400 [b]	1450	480	3.02
Coach [c]	254	110	2.32
Maglev [d]	227	430	0.527
Train [d]	184	300	0.612
STV [e]	130	1500	0.0865

[a] V_0 is the fixed vehicle speed at which the un-normalized energy consumption E_0 was measured or calculated. [b] From Table 4. Speed of 870 km/h for the Boeing 747 at altitude of 10 700 m (see Table 4) corresponds to Mach 0.81. [c] From Table 3. [d] From Ref. [20]. [e] From Ref. [1]

Table 3 – Empirical data for coach energy analysis

Source	Seats N_0	Cruise Speed V_0 mi/h	Fuel Consumption [a] mi/gal
Custom Coach Corp [b]	53	65	6-7
Arrow Stage Lines [c, d]	56	68	6.1-6.4
Ramblin Express [e]	56	70	6.5
Mean:	**55**	**68**	**6.4**

[a] Diesel fuel

[b] Manufacturer of coaches [17]

[c] Ref. [19]

[d] The midpoint of the reported range of fuel consumption values, namely, 6.25 mi/gal, was used in the computation of the mean over the three data sets

[e] Several makes of coaches, including MCI and Prevost [18]

Table 4 – Empirical data[a] for airplane energy analysis

Airplane	Mean Seats	Mean Cruise Speed mi/h	Mean Fuel Consumption [b] gal/seat
Boeing 747-400[c]	371	539	84.32
Bombardier Q400[d]	74	299	4.82

[a] Data from reference [22]

[b] Jet A fuel for all airplanes

[c] Boeing 747-400 data were compiled from 4773 flights of two US carriers between the US and Asia/Oceania and some within Asia/Oceania (e.g., Tokyo to Hong Kong). These comprise all such flights of the two carriers during the third quarter of 2008. Mean distance from gate-to-gate was 4777 miles (7690 km), and mean altitude was estimated as 35 thousand feet (10 700 m). The Boeing 747-400 for these routes has only two seating configurations (to accommodate multiple fare classes), and the number of seats is the average over all flights. Mean cruise speed was computed by dividing mean gate-to-gate distance by mean takeoff-to-landing flight time of 8.86 h.

[d] Bombardier Q400 data were compiled from 23 758 flights of one US carrier within the US mainland. These comprise all such flights of the carrier during the third quarter of 2008. Mean distance from gate-to-gate was 287 miles (462 km), and mean altitude was estimated as 25 thousand feet. The Q400 has a single fare class with 74 seats. Mean cruise speed was computed by dividing mean gate-to-gate distance by mean takeoff-to-landing time of 0.960 h.